Photocrystallography

DOI: 10.1002/anie.200805997

Photomagnetic Switching of the Complex $[Nd(dmf)_4(H_2O)_3(\mu\text{-}CN)Fe(CN)_5]\cdot H_2O$ Analyzed by Single-Crystal X-Ray Diffraction**

*Helle Svendsen, Jacob Overgaard, Marie Chevallier, Eric Collet, and Bo B. Iversen**

Controlling the physical properties of materials with light irradiation represents an emerging field involving many different types of photoswitchable molecular systems. The photoswitching involves not only electronic excitation, but also a coupling with the structural degrees of freedom, which play a key role in stabilizing the excited state from μs to days. In concert with these developments, photocrystallography has become a rapidly evolving branch of modern crystallography, which provides unique experimental access to structural information for molecules in electronically excited states.[1] In the case of very short lifetimes (< ms) time-resolved diffraction is needed, whereas for long-lived states normal diffraction experiments can be carried out (steady-state method).[2] The first compound to be studied by a steady-state photoinduced method was $Na_2[Fe(CN)_5(NO)]\cdot 2H_2O$, which has a ligand isomerization effect.[3,4] Another type of photoisomerization was detected in several $\{Ru{-}SO_2\}$ complexes.[5,6] Structural changes were detected in iron-containing complexes with light-induced excited spin-state trapping (LIESST) properties.[1b,d–e] Extension of this work to a dinuclear spin-crossover compound demonstrated that in such a three-state system (LS–LS, HS–LS and HS–HS) one can selectively switch between different states by tuning the laser excitation wavelength.[7] Beyond structural reorganization, electron redistribution in a photoinduced excited HS state was recently reported.[8] At the other end of the time scale, microsecond time-resolved diffraction experiments have been carried out on, for example, $[Pt_2(H_2P_2O_5)_4]^{4-}$, for which a decrease in the Pt–Pt bond length was found.[9] Structures with lifetimes from picoseconds to nanoseconds have also been investigated, and, as an example, a photoinduced paraelectric (neutral) to ferroelectric (ionic) structural phase transition was detected in tetrathiafulvene–*p*-chloranil on the picosecond timescale.[10]

One material property of particular interest is photoinduced magnetization, especially in relation to the development of new memory devices.[11] For example, Li et al. showed that a cyanide-bridged heterobimetallic complex containing neodymium and iron, $[Nd(dmf)_4(H_2O)_3(\mu\text{-}CN)Fe(CN)_5]\cdot H_2O$ (**1**; Figures 1 and 2; dmf = *N*,*N*-dimethylformamide), underwent a surprisingly large increase in magnetic susceptibility upon illumination with UV light at low temperatures ($T <$ 50 K).[12]

The nature of the electronic transition, which caused this change in the magnetic properties of **1**, is not known, and it is of considerable interest to explore any significant structural changes in the excited state, which may explain the structural

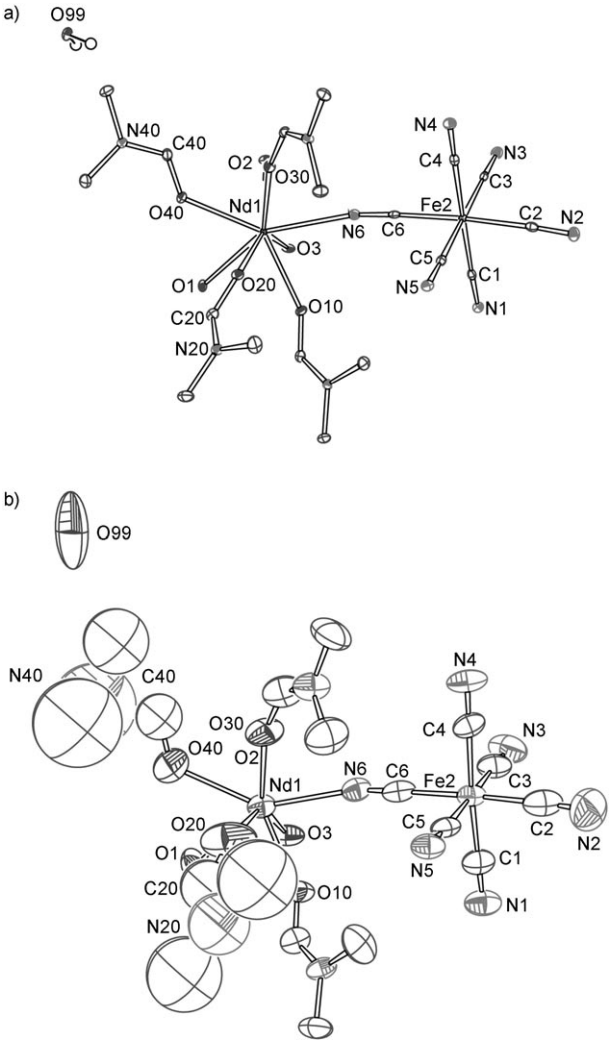

Figure 1. Molecular structure of **1** at 15 K. Thermal ellipsoids are drawn at 50% probability, and H atoms are omitted from the main molecule for clarity; a) ground-state structure (data collection 0); b) excited-state structure (data collection 7).

[*] H. Svendsen, Dr. J. Overgaard, M. Chevallier, Prof. Dr. B. B. Iversen
Centre for Energy Materials, Department of Chemistry and iNANO
University of Aarhus, 8000 Århus C (Denmark)
Fax: (+45) 8619-6199
E-mail: bo@chem.au.dk
Prof. E. Collet
Institut de Physique de Rennes, Université de Rennes 1
UMR UR1-CNRS 6251, 35000 Rennes (France)

[**] The authors gratefully acknowledge the beam time obtained at the ChemMatCARS beam line at APS, Argonne National Laboratory. The work was supported by DANSCATT. Dr. Yu-Sheng Chen is thanked for assistance during measurements.

Supporting information for this article is available on the WWW under http://dx.doi.org/10.1002/anie.200805997.

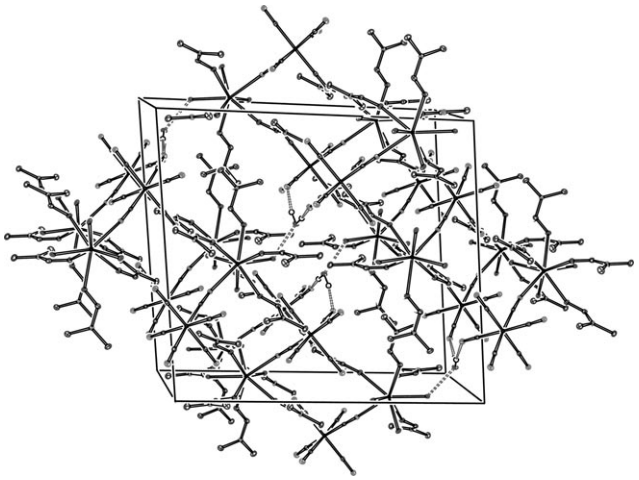

Figure 2. Packing of **1** in the ground state. Thermal ellipsoids are drawn at 50% probability, and H atoms for the main molecules are omitted for clarity.

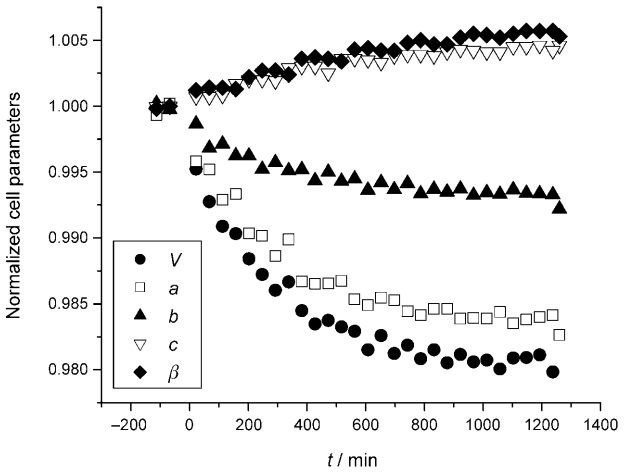

Figure 3. Unit-cell parameters as a function of time. The laser is turned on at $t = 0$ min. The standard deviation values are smaller than the symbols used in the plot. Unit-cell parameters have been calculated for each of the 32 separate ω scans.

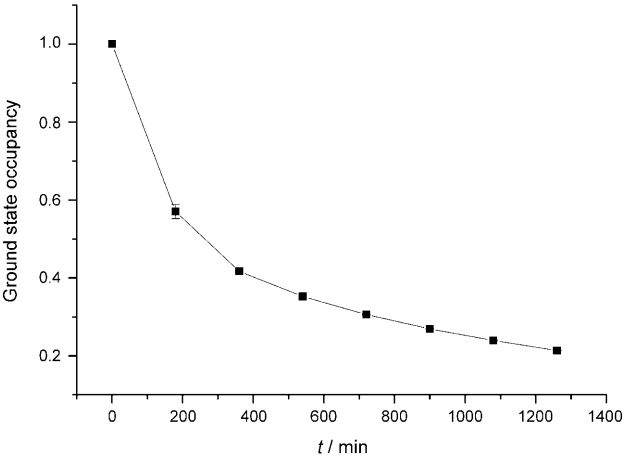

Figure 4. Occupancy of the ground state as a function of time. The laser is turned on only after the first data point has been made.

trapping of the excited state. This can reveal which part of the molecule is involved in the electronic transition and possibly provide an explanation for the photo-induced magnetism. According to Li et al., the excited state of **1** is metastable with a lifetime of several hours at temperatures below 50 K, making it possible to measure both the ground state and the excited state structures using conventional low-temperature crystallographic techniques. Herein we report such photocrystallographic investigations of **1**, in which a complete single-crystal X-ray data set was collected every three hours on a crystal kept at 15 K. The first data set was measured without UV light, whereas the remaining seven data sets were collected with continuous illumination (see the Experimental Section). A number of isostructural complexes with metal substitution as well as related complexes[13] are currently under investigation in our group.

Normalized unit-cell parameters are plotted as a function of time (Figure 3). Significant changes in the unit-cell parameters led to a total decrease in the volume of approximately 2% after seven data collections (ca. 22 h). The changes were much larger than the experimental uncertainties, thereby strongly indicating that the crystal was successfully photoexcited. The unit cell changes did not occur instantaneously, but seemed to be slowly induced as a function of time. Even after 22 h, the cell parameters were still slowly changing, indicating that full saturation had not been completely achieved.

Occupancy of the ground state as a function of time was determined by refining a model containing two molecular conformers (Figure 4). The photoconversion was not complete after 24 h and it may not reach higher than 80% with the current setup, which differs significantly from the original setup by Li et al., who used a powder sample.[12]

The structural data revealed significant bond-length changes (up to eight estimated standard deviations (esds)) upon excitation. Metal–ligand and cyano bond lengths for both molecular states are shown in Table 1. The largest changes were found around the Fe center with a maximal decrease of approximately 4.3% (corresponding to 0.083 Å) for the Fe–C3 bond. The changes around the Nd atom are also large, with a 3.2% decrease for the Nd–N6 bond (0.081 Å). At the same time the Nd–O40 bond length increases significantly. Interestingly, all C≡N bond lengths increase except for the one which connects the two metal sites, for which no change takes place. With one exception, no other significant bond-length changes occur in the rest of the molecule: The exception is, perhaps surprisingly, two of the DMF groups, which are located far from the metal centers. The DMF molecules are completely ordered in the ground-state structure, but in the excited-state structure, the atoms in the two DMF groups show unusually large cigar-shaped thermal ellipsoids. Large ellipsoids are typically a sign of structural disorder, but we have not been able to refine a DMF model with two conformations. Overall, there is a significant and fairly uniform increase in the atomic displacement parameters (ADPs) on all atoms of the excited state structure, but the average ADP differences, ΔU, along the bonding directions (Hirshfeld test) only undergo a modest increase (see the Supporting Information). The large ADPs in the excited-state structure could be a result of an over-

Table 1: Metal–ligand and C≡N bond lengths in the ground state (refinement of data collection 0) and the excited state (refinement of data collection 7). The ratio between the ground-state and excited-state bond lengths is also given.

Bond	Ground-state bond length [Å]	Excited state bond length [Å]	Ratio ES/GS	Change [%]
Nd–N6	2.557(2)	2.476(6)	0.968(2)	−3.2(2)
Nd–O1	2.459(1)	2.481(5)	1.009(2)	0.9(2)
Nd–O2	2.451(1)	2.431(4)	0.992(2)	−0.8(2)
Nd–O3	2.479(1)	2.479(4)	1.000(2)	0.0(2)
Nd–O10	2.421(1)	2.384(5)	0.985(2)	−1.5(2)
Nd–O20	2.432(1)	2.454(6)	1.009(3)	0.9(3)
Nd–O30	2.401(1)	2.364(5)	0.985(2)	−1.5(2)
Nd–O40	2.439(1)	2.539(6)	1.041(3)	4.1(3)
Fe–C1	1.935(2)	1.891(8)	0.977(4)	−2.3(4)
Fe–C2	1.939(2)	1.866(10)	0.962(5)	−3.8(5)
Fe–C3	1.946(2)	1.863(9)	0.957(5)	−4.3(5)
Fe–C4	1.939(2)	1.897(7)	0.978(4)	−2.2(4)
Fe–C5	1.943(2)	1.911(8)	0.984(4)	−1.6(4)
Fe–C6	1.945(2)	1.930(8)	0.992(4)	−0.8(4)
C1–N1	1.157(2)	1.178(8)	1.018(7)	1.8(7)
C2–N2	1.159(2)	1.195(10)	1.031(9)	3.1(9)
C3–N3	1.154(2)	1.200(9)	1.040(8)	4.0(8)
C4–N4	1.152(2)	1.165(8)	1.011(7)	1.1(7)
C5–N5	1.152(2)	1.160(8)	1.007(7)	0.7(7)
C6–N6	1.155(2)	1.151(8)	0.997(7)	−0.4(7)

estimated occupancy parameter. Thus, the precise occupancy value in each data collection could be slightly in error. However, the relative changes between data collections should be reliable, and indeed the smoothness of the curve in Figure 4 is very convincing.

The main tendency is for metal–ligand bond lengths to decrease in the excited state, whereas C≡N bond lengths increase.

To date, no precise explanation has been given for the photomagnetic effect in **1**. Since the susceptibility increased upon UV illumination, a process increasing the magnetic moment must have taken place. There are two possible explanations for this. The first is that more unpaired spins were introduced on the iron or neodymium ions, either by metal-to-metal charge transfer (MMCT), ligand-to-metal charge transfer (LMCT), or spin crossover from a low-spin to a high-spin configuration. A second explanation is a change in the coupling between Nd and Fe, which is known to be antiferromagnetic.[14] The excitation may strengthen the 3d–4f coupling or even change it to a ferromagnetic coupling.

MMCT was ruled out based on analysis of Mössbauer spectroscopy data by Li et al.[12] Furthermore, a decrease in the quadrupole splitting suggested a possible distortion of the $\{Fe^{III}(CN)_6\}$ moiety, and UV/Vis and IR spectra indicated an increase in the electron density on Fe^{III}. Since the largest bond-length changes occur around the iron atom, it is reasonable to believe that iron is involved in the excitation process. Therefore, an LMCT on Nd is unlikely. Furthermore, no spin change can take place on Nd, which presumably has a high-spin (HS) configuration. On Fe, a transformation from a low-spin (LS) to a HS configuration would lead to a population of the antibonding e_g orbitals, which would increase the metal–ligand bond lengths, as observed for spin-crossover systems. This is therefore not a plausible explanation in the case of **1**. A LMCT on the iron ion was postulated by Li et al. to be the result of the UV illumination. The Fe^{2+}–L bond lengths are often longer than Fe^{3+}–L bond lengths.[15] However, owing to strong back donation from the cyano ligands to iron, which makes the t_{2g} orbitals bonding, Fe^{2+}–C bond lengths are generally shorter than Fe^{3+}–C bond lengths in an $\{Fe(CN)_6\}$ entity.[16] Thus, when going from Fe^{3+} to Fe^{2+} the population of the t_{2g} orbitals will increase, and the bond lengths decrease. The present excited-state structure clearly shows a decrease in the iron–ligand bond lengths, and this makes the LMCT effect on iron a possible cause of the photomagnetic effect. This idea is also corroborated by the increase in the cyano bond lengths. It should be noted that only the first stages of LMCT processes are purely electronic excitations. Important coupling with the structural degrees of freedom may populate a low-lying energetic state of different nature, as in the case of LIESST for which the change of spin state does not directly occur through the forbidden optical process. The photo-excitation could also introduce a change in the 3d–4f intramolecular magnetic coupling. This hypothesis is supported by the clear structural changes in the excited state which has longer CN bonds and shorter Fe–C bonds, as well as a shorter Nd–N6 bond, all in all creating a shorter path between the two interacting metal centers. The distance between the two metal centers through the cyano group decreases from 5.657 Å in the ground state to 5.557 Å in the excited state. Based on the arguments above it seems that the photo-excitation could either be caused by a LMCT on iron or a change in the 3d–4f intramolecular magnetic coupling. At the moment it is not clear, which one of the two is the cause of the observed photomagnetic effect

In summary, single-crystal X-ray diffraction experiments have revealed the excited state structure of the photomagnetic hetero-bimetallic complex **1**. Clear structural changes were detected, with a decrease in all metal–ligand bond lengths. The largest modifications were in the iron–ligand bond lengths, which strongly indicates that the iron atom plays an important role in the excitation process. However, unlike typical changes for LS to HS processes, the present system shows a decrease in all iron–ligand bond lengths which could indicate a LMCT to take place on iron or that photoexcitation involves a change in the superexchange coupling between the metal centers. Significant structural changes also took place for two DMF ligands located on the back side of the molecule, far away from the iron center. The significance of this photoinduced structural disorder remains to be clarified. It should also be noted that, in the crystal, the molecular units are interconnected by quite strong hydrogen bonds through the solvated water molecule. The effect of this supramolecular network also requires further study. Further photocrystallographic studies of isostructural metal-substituted compounds as well as ab initio calculations are in progress to obtain a deeper understanding of the photomagnetic process taking place in **1**.

Experimental Section

Synthesis of $[Nd(dmf)_4(H_2O)_3(\mu\text{-}CN)Fe(CN)_5]\cdot H_2O$ (**1**): A solution of $NdCl_3$ (1 mmol) in DMF (5 mL) was added very slowly (down the side

of the glass) to a solution of $K_3[Fe(CN)_6]$ (1 mmol) in water (10 mL). Green-yellow crystals precipitated out and after evaporation the crystals were suitable for single-crystal X-ray diffraction. **1** crystallized in the monoclinic space group $P2_1/n$ with four asymmetric $[Nd(C_3H_7NO)_4Fe(CN)_6]\cdot H_2O$ units per unit cell. The molecules bonded to each other with strong hydrogen bonds through the cocrystallized water molecule (Figure 2).

Photocrystallography: Single-crystal X-ray diffraction experiments with and without UV illumination were carried out at the University of Rennes, France, using $Mo_{K\alpha}$ radiation on an Oxford Diffraction Xcalibur3 diffractometer equipped with a CCD detector. The dimensions of the crystal were ca. 150 μm, and it was attached with oil on a goniometer head before mounting on the diffractometer. Data were collected at 15 K using a HeliJet cryocooler, and the light source was a UV diode with an emission wavelength of 390 ± 10 nm. The diode was held fixed during the entire experiment, and the light was focused on the crystal by a lens. The excitation density at the crystal was around $100\,mW\,cm^{-2}$. A ground-state data collection consisting of four different ω scans and lasting approximately 3 h was made prior to turning on the UV diode (data collection 0). After turning on the laser diode, the exact same data collection was repeated seven times before the helium tank was eventually depleted. Each 3 hour data set was analyzed independently to follow structural changes as a function of time. The data collection and reduction were performed with the programs CrysAlis CCD and CrysAlis RED.[17] No absorption correction was performed ($\mu = 2.24\,mm^{-1}$). The structures were refined with SHELXL-97,[18] and all non-water hydrogen atoms were refined as riding on the parent C atom.[19] The ground-state data collection (data collection 0) was refined using a single conformer with full occupancy on all sites, and all atoms except hydrogen were treated anisotropically. The ground-state fractional coordinates and ADPs were then imported into the refinement of the last data collection (data collection 7), where two conformers were refined; an excited-state structure and a fixed ground-state structure, and the sum of their occupancies was kept fixed at unity. Restraints were imposed on the bond lengths in the DMF ligands in the excited state, and the atoms in the DMF groups 20 and 40, together with all hydrogen atoms, were refined isotropically. All other atoms in the excited-state conformer were refined with anisotropic atomic displacements parameters. The structural model of the excited state (fractional coordinates and ADPs) obtained from data collection 7 and the ground-state model were then imported and kept fixed in the refinements of the remaining 6 data collections (data collection 1–6); only the scale factor and the occupancy factor were refined. An analysis of the data using only one "average" conformer has also been performed. This model showed the exact same tendencies for the changes in the bond lengths in the excited state as those obtained from the two conformer model (although the changes were smaller). To investigate the reversibility of the photomagnetic effect, the crystal was taken out of the cold stream and UV light after the last data collection, but unfortunately the crystal did not survive this treatment.

CCDC 703614, 703615, 703616, 703617, 703618, 703619, 703620, 703621, 703757, 703758 contain the supplementary crystallographic data for this paper. These data can be obtained free of charge from The Cambridge Crystallographic Data Centre via www.ccdc.cam.ac.uk/data_request/cif.

Received: December 9, 2008
Revised: February 24, 2009
Published online: March 6, 2009

Keywords: heterometallic complexes · magnetic properties · photocrystallography · structure elucidation · X-ray diffraction

[1] a) P. Coppens, I. Novozhilova, A. Kovalevsky, *Chem. Rev.* **2002**, *102*, 861–883; b) P. Coppens, *Chem. Commun.* **2003**, 1317–1320; c) J. M. Cole, *Acta Crystallogr. Sect. A* **2008**, *64*, 259–271; d) K. Ichiyanagi, J. Herbert, L. Toupet, H. Cailleau, P. Guionneau, J.-F. Létard, E. Collet, *Phys. Rev. B* **2006**, *73*, 060408; e) V. Legrand, S. Pillet, C. Carbonea, M. Souhassou, J.-F. Létard, P. Guionneau, C. Lecomte, *Eur. J. Inorg. Chem.* **2007**, 5693–5706.

[2] J. M. Cole, *Chem. Soc. Rev.* **2004**, *33*, 501–513.

[3] M. Rüdlinger, J. Schefer, T. Vogt, T. Woike, S. Haussühl, H. Zöllner, *Physica B* **1992**, *180*, 293–298.

[4] M. D. Carducci, M. R. Pressprich, P. Coppens, *J. Am. Chem. Soc.* **1997**, *119*, 2669–2678.

[5] a) A. Y. Kovalevsky, K. A. Baglet, P. Coppens, *J. Am. Chem. Soc.* **2002**, *124*, 9241–9248; b) A. Y. Kovalevsky, K. A. Baglet, J. M. Cole, P. Coppens, *Inorg. Chem.* **2003**, *42*, 140–147.

[6] K. F. Bowes, J. M. Cole, S. L. G. Husheer, P. R. Raithby, T. L. Savarese, H. A. Sparkes, S. J. Teat, J. E. Warren, *Chem. Commun.* **2006**, 2448–2450.

[7] E. Trzop, M. B. L. Cointe, H. Cailleau, L. Toupet, G. Molnar, A. Bousseksou, A. B. Gaspar, J. A. Real, E. Collet, *J. Appl. Crystallogr* **2007**, *40*, 158–164.

[8] S. Pillet, V. Legrand, H. P. Weber, M. Souhassou, J.-F. Létard, P. Guionneau, C. Lecomte, *Z. Kristallogr.* **2008**, *223*, 235–249.

[9] a) C. D. Kim, S. Pillet, G. Wu, W. K. Fullagar, P. Coppens, *Acta Crystallogr. Sect. A* **2002**, *58*, 133–137; b) Y. Ozawa, M. Terashima, M. Mitsumi, K. Toriumi, N. Yasuda, H. Uekusa, Y. Ohashi, *Chem. Lett.* **2003**, *32*, 62–63; c) N. Yasuda, M. Kanazawa, H. Uekusa, Y. Ohashi, *Chem. Lett.* **2002**, 1132–1133.

[10] E. Collet, M.-H. Lemée-Cailleau, M. B.-L. Cointe, H. Cailleau, M. Wulff, T. Luty, S.-Y. Koshihara, M. Meyer, L. Toupet, P. Rabiller, S. Techert, *Science* **2003**, *300*, 612–615.

[11] Y. Einaga, *J. Photochem. Photobiol. C* **2006**, *7*, 69–88.

[12] G. Li, T. Akitsu, O. Sato, Y. Einaga, *J. Am. Chem. Soc.* **2003**, *125*, 12396–12397.

[13] a) J. Overgaard, H. Svendsen, M. A. Chevallier, B. B. Iversen, *Acta Crystallogr. Sect. E* **2005**, *61*, 268–270; b) H. Svendsen, J. Overgaard, M. A. Chevalier, B. B. Iversen, *Acta Crystallogr. Sect. E* **2006**, *62*, 989–991.

[14] A. Figuerola, C. Diaz, J. Ribas, V. Tangoulis, J. Granell, F. Lloret, J. Mahía, M. Maestro, *Inorg. Chem.* **2003**, *42*, 641–649.

[15] See for example, a) J. Overgaard, F. K. Larsen, B. Schiøtt, B. B. Iversen, *J. Am. Chem. Soc.* **2003**, *125*, 11088–11099; b) C. Wilson, B. B. Iversen, F. K. Larsen, J. Overgaard, G. Wu, S. P. Palii, G. A. Timco, N. V. Gerbeleu, *J. Am. Chem. Soc.* **2000**, *122*, 11370–11379.

[16] See for example, a) R. Haser, C. E. De Broin, M. Pierrot, *Acta Cryst.* **1972**, *B28*, 2530–2537; b) P. M. Pierrot, R. Kern, R. Weiss, *Acta Cryst.* **1966**, *20*, 425–428.

[17] Oxford Diffraction, CrysAlis CCD and CrysAlis RED., Oxford Diffraction L.td, Abingdon, Oxfordshire, England, **2007**.

[18] SHELX-97—Programs for Crystal Structure Analysis (Release 97-2). Sheldrick, G. M., Institüt für Anorganische Chemie der Universität Göttingen, Tammanstrasse 4, D-3400 Göttingen, Germany, **1998**.

[19] Data collection 0: Space group $P2_1/n$; $a = 17.6790(4)$, $b = 8.837(2)$, $c = 19.445(4)$ Å; $\beta = 96.25(3)°$; $V = 3019.7(11)$ Å^3; 28472 reflections measured; 9687 unique reflections ($R_{int} = 0.0286$); Refinement: $N_{obs}(I>2\sigma) = 7307$, $N_{par} = 367$, $N_{restraints} = 12$, $R_{all} = 0.0389$, $R(I>2\sigma) = 0.0236$, $wR(I>2\sigma) = 0.0475$. Data collection 7: Space group $P2_1/n$; $a = 17.4155(8)$, $b = 8.7848(4)$, $c = 19.5099(9)$ Å; $\beta = 96.679(4)°$; $V = 2964.6(2)$ Å^3; 27542 reflections measured; 9968 unique reflections ($R_{int} = 0.0832$); Refinement: $N_{obs}(I>2\sigma) = 3515$, $N_{par} = 304$, $N_{restraints} = 28$, $R_{all} = 0.1655$, $R(I>2\sigma) = 0.0462$, $wR(I>2\sigma) = 0.0841$.

